An Exploration of CHRIS PROBA Hyperspectral Imagery for Obtaining Burnt Area Cartography From a Uni-temporal Perspective

George P. Petropoulos[∫], Charalambos Kontoes[§]

[∫] Institute of Geography and Earth Sciences, University of Aberystwyth, Wales, United Kingdom

[§]. Institute of Space Applications and Remote Sensing, National Observatory of Athens, Greece

Contact: george.petropoulos@aber.ac.uk

1. INTRODUCTION:

Wildland fires have long been considered as one of the most threatening disturbance factors, for properties, infrastructures as well as ecosystems. Being able to obtain accurate as well as rapid mapping of burnt areas shortly after fire suppression, among others is of key importance in policy decision making, modeling the atmospheric and climatic impacts of burnt biomass, as well as in estimating the total atmospheric emissions deriving from it (*Rosa et al., 2008;Petropoulos et al., 2012*).

With the support of modern technologies, such as of **Earth Observation (EO)** and combined with **Geographical Information Systems (GIS)**, today's societies are able to map and analyse wildland fires at large observational scales and at inaccessible locations in a cost-effective, repetitive and systematic way. The recent technological advances in EO technology have resulted to the development of hyperspectral systems, which collect spectral information in a large number of discrete, narrow spectral bands. As a result, those provide very rich spectrally information content that enhances dramatically our ability to accurately identify different targets on the Earth's surface.

This study evaluates the use of **CHRIS-PROBA** hyperspectral imagery in burnt area extraction when combined with advanced pixel-based classifiers developed herein.

2 STUDY SITE:

As a case study it was selected a fire occurred in the summer of 2007 in the island of Evoia, located near the capital of Greece.

Selection of the site was based on the availability of satellite observations from *CHRIS-PROBA*, acquired shortly after the fire suppression, and the importance of assessing the burning for the wider region.

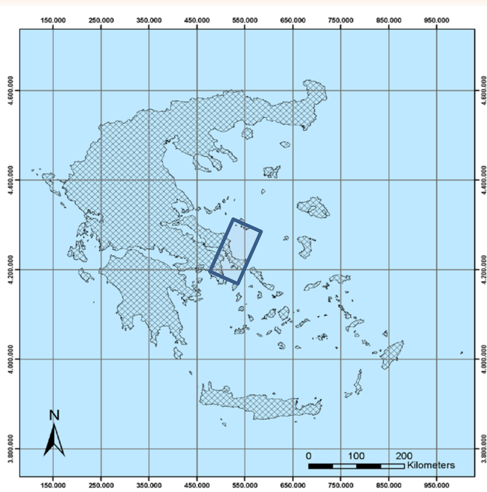

Fig. 1: *Study site location*

3. DATASETS:

CHRIS Instrument Specifications:

- ✓ *Hyperspectral instrument onboard PROBA platform operated from ESA*
- ✓ *Up to 5 different viewing angles*
- ✓ *19 spectral bands (fully programmable) in the VNIR range (400 - 1050 nm)*
- ✓ *Spatial resolution of 17m*
- ✓ *Can be configured to provide 63 spectral bands at a spatial resolution of ~34 m.*

DATASETS:

- ➢ ***CHRIS PROBA*** *(September 1st, 2007), at no cost from EOLiSA*
- ➢ ***CORINE*** *2000 (100m)*
- ➢ ***Burnt area estimate from RiskEOS operational service*** *(Services and Applications for Emergency Response developed in the framework of GMES-SE of ESA.*

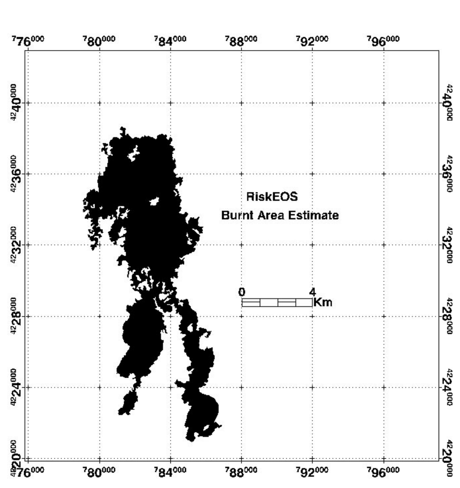

Fig. 2a: *RiskEOS BA dataset*

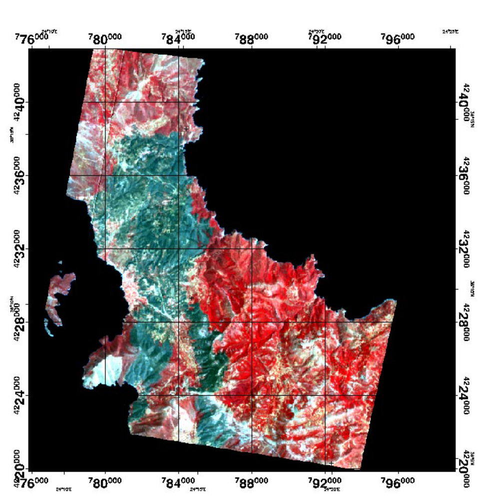

Fig. 2b: *CHRIS image acquired (FCC)*

4. METHODS:

ANN classifier: *Learning occurs by adjusting the weights in the nodes to minimise difference between the output node activation and the output (Atkinson et al., 1997)*

SVMs classifier: separates the classes with a decision surface (*optimal hyperplane*) that maximizes the margin between the classes. Points closest to hyperplane are the *support vectors (Vapnik, 1999)*

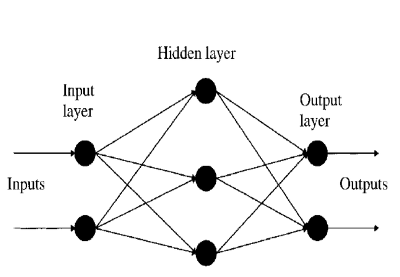

Fig. 3: *ANN structure (here with 1 hidden layer)*

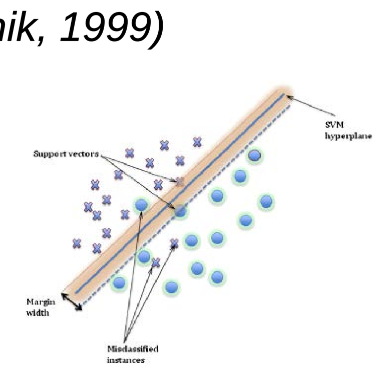

Fig. 4: *SVMs operation*

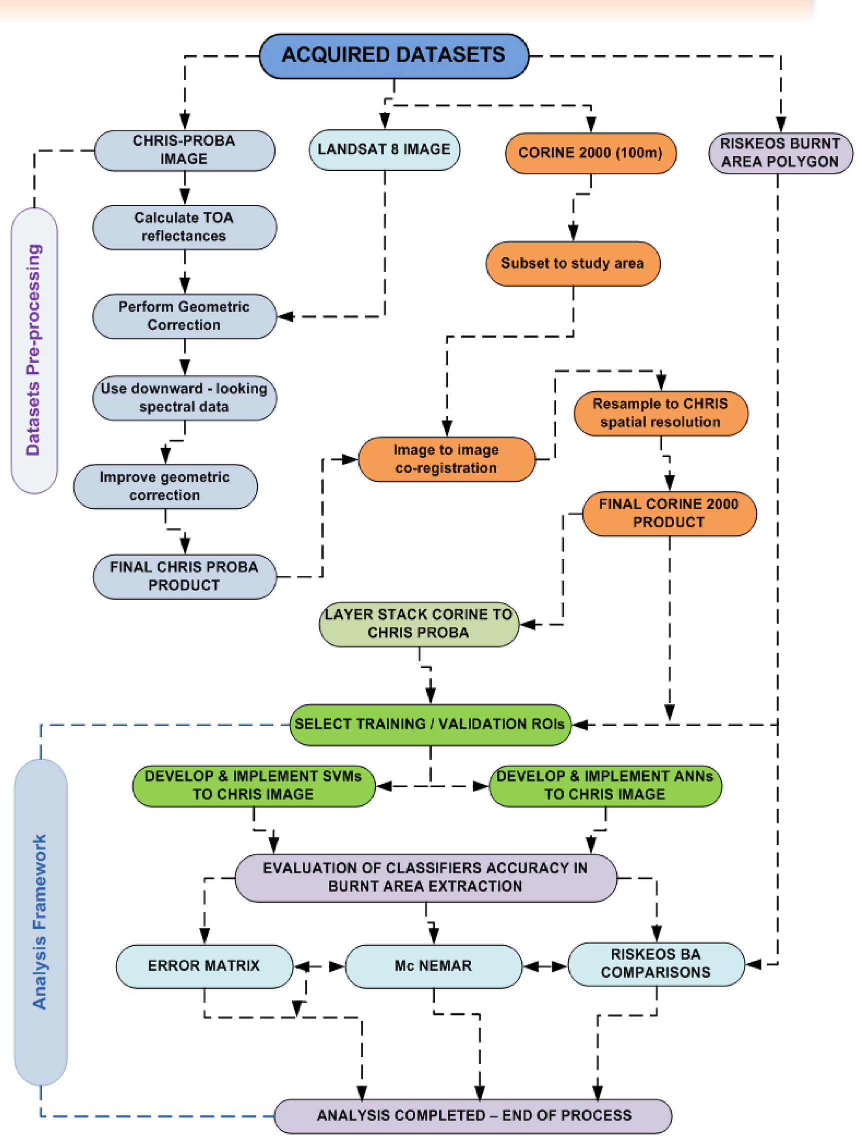

Fig. 5: *Overall methodology followed*

5. RESULTS:

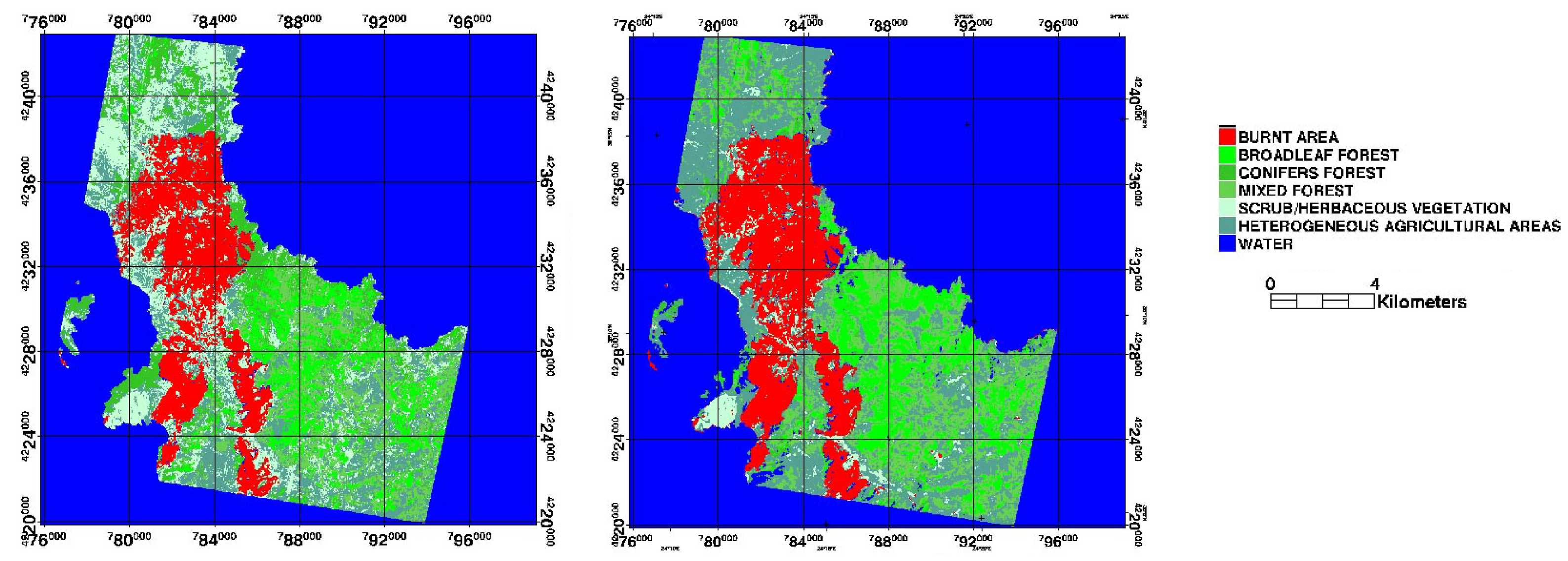

Fig. 6: *CHRIS PROBA classification using ANNs (left) and SVMs (right) classifiers*

Table 1: *Classification accuracy measures obtained using the same set of validation points*

	ARTIFICIAL NEURAL NETWORKS		SUPPORT VECTOR MACHINES	
	UA (%)	PA (%)	UA (%)	PA (%)
Burnt Area class	*98.15*	*97.87*	*98.88*	*99.14*
Overall Accuracy	*86.18*		*94.93*	
Kappa Coefficient	*0.829*		*0.937*	

Table 2: *McNemar statistical analysis results*

f_{11}: number of cases with correct classification in both maps;
f_{12}: number of cases that are correctly classified by SVMs but incorrectly by ANNs
f_{21}: number of cases that are correctly classified ANNs, but incorrectly by SVMs
f_{22}: number of cases that are wrongly classified by both ANNs & SVMs

Classification method	f_{11}	f_{12}	f_{21}	f_{22}	Total	P-value
Artificial Neural Networks	226	19	4	12	261	<0.001
Support Vector Machines	232	21	2	7	262	<0.001

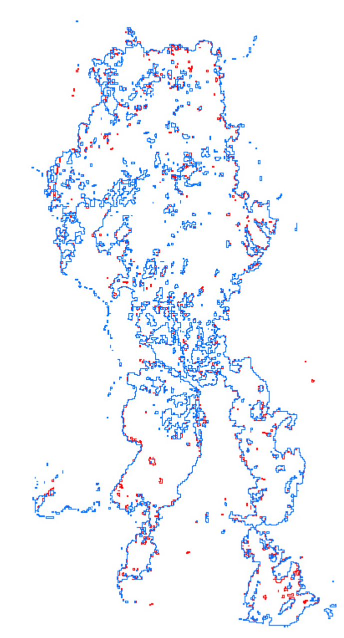

Fig. 7: *CHRIS PROBA burnt area estimated from ANN (red), SVMs (blue).*

Table 3: *CHRIS-predicted burnt area estimates against the RiskEOS*

CLASSIFICATION METHOD	Common burnt area between CHRIS & SAFER (DBA)	False burnt areas (FBA)	Skipped Burnt areas (SBA)	Detection Efficiency rate[DBA/(DBA+SBA)]	Commission Error (False Alarm rate) [FBA/(DBA+FBA)]	Omission Error (Skipped Area rate) [SBA/(DBA+SBA)]
CHRIS_ANNs	46.89	17.65	12.41	0.791	0.274	0.209
CHRIS_SVMs	51.53	9.14	6.51	0.888	0.151	0.112

6. CONCLUSIONS:

❑ . Overall, results exemplified the appropriateness of the spatial and spectral resolution of CHRIS sensor in obtaining rapid and cost-effective post-fire analysis.

❑. SVMs outperformed the ANNs classifier in terms of both overall accuracy and BA mapping as indicated by classification accuracy measures. Also total burnt area estimate from SVMs was generally in closer agreement with the SAFER validated estimate. Results obtained were also found statistically significant.

❑. Results are comparable to other studies implemented in other regions using both multispectral and hyperspectral data using both ANNs & SVMs.

❑. Differences obtained are attributed mainly to the algorithms characteristics on treatment of land cover heterogeneity and terrain complexity. Though, misclassifications observed in both cases, which may in part attributed to spectral mixing effects

❑. It appears that if hyperspectral technology is incorporated into the operational development of services for the estimation of burnt areas, the resulting combination has the potential to prove highly useful in producing enhancing the thematic accuracy of mapping and advancing the thematic content of the fire recovery operational products such as that produced in the framework of RiskEOS operational service.

References:

Petropoulos, G.P., C. C. Kontoes, and I. Keramitsoglou, 2012. Land cover mapping with emphasis to burnt area delineation using co-orbital ALI and Landsat TM imagery. International Journal of Applied Earth Observation and Geoinformation, 18, 344-355. **Kontoes C.C., Poilvé H., Florsch G., Keramitsoglou I., Paralikidis S., 2009.** A Comparative Analysis of a Fixed Thresholding vs. a Classification Tree Approach for Operational Burn Scar Detection and Mapping, International Journal of Applied Earth Observation and Geoinformation, 11, 23-41.**Rosa De La J. M., Gonzalez-Perez, J.A., Gonzalez-Vazquez, R., Knicer, H. , Lopez-Capel, E., Manning, D.A.C. and F.J. Gonzalez-Vila, 2008.** Use of pyrolisis/GC-MS combined with thermal analysis to monitor C and N changes in soil organic matter from a Mediterranean fire affected forest. Catena, 74, 296-303. **Vapnik, V. 1998.** Statistical Learning Theory, Wiley, New York. **Atkinson, P.M. and Tatnall, A.R. 1997.** "Introduction: neural networks in remote sensing," Intern. Journal of Remote Sensing, 1997, vol. 18, pp. 699-709

Acknowledgments:

Authors are grateful to ESA for making available at no cost the CHRIS-PROBA imagery as well as the RiskEOS for the provision of their burnt area estimate.